Clinical and Experimental Immunology, 2024, **216**, 113–119
https://doi.org/10.1093/cei/uxad085
Advance access publication 28 July 2023
Research Article

Clinical & Experimental IMMUNOLOGY

OXFORD

Research Article

Clinical and cellular phenotypes resulting from a founder mutation in *IL10RB*

Zhiming Mao[1,‡], Michael J. Betti[2,‡], Miguel A. Cedeno[3], Luis A. Pedroza[4], Shamel Basaria[5], Qi Liu[5], Joseph M. Choi[5], Janet G. Markle[2,5,*]

[1]Department of Molecular Microbiology and Immunology, Johns Hopkins Bloomberg School of Public Health, Baltimore, MD, USA
[2]Division of Genetic Medicine, Department of Medicine, Vanderbilt University Medical Center, Nashville, TN, USA
[3]Department of Pediatrics, Hospital de ninos Roberto Gilbert Elizalde, Guayaquil, Ecuador
[4]Department of Pediatrics, Vagelos College of Physicians and Surgeons, Columbia University Irving Medical Center, New York, NY, USA
[5]Division of Molecular Pathogenesis, Department of Pathology Microbiology and Immunology, Vanderbilt University Medical Center, Nashville, TN, USA

[‡]Equal contributions.
[*]Correspondence: Janet G. Markle, Division of Molecular Pathogenesis, Department of Pathology Microbiology and Immunology, Vanderbilt University Medical Center, Nashville, TN, USA. Email: janet.markle@vumc.org

Abstract

Inborn errors of immunity are a group of rare genetically determined diseases that impair immune system development or function. Many of these diseases include immune dysregulation, autoimmunity, or autoinflammation as prominent clinical features. In some children diagnosed with very early onset inflammatory bowel disease (VEOIBD), monogenic inborn errors of immune dysregulation underlie disease. We report a case of VEOIBD caused by a novel homozygous loss of function mutation in *IL10RB*. We use cytometry by time-of-flight with a broad panel of antibodies to interrogate the immunophenotype of this patient and detect reduced frequencies of CD4 and CD8 T cells with additional defects in some populations of T helper cells, innate-like T cells, and memory B cells. Finally, we identify the patient's mutation as a founder allele in an isolated indigenous population and estimate the age of this variant by studying the shared ancestral haplotype.

Keywords: IL-10, inflammatory bowel disease, founder mutation

Abbreviations: B-LCL: B-lymphocytic cell line; CyTOF: cytometry by time-of-flight; DP T cells: double-positive T cells; HSCT: hematopoietic stem cell transplantation; MAIT: mucosal-associated invariant T cells; PBMC: peripheral blood mononuclear cell; VEOIBD: very early onset inflammatory bowel disease.

Introduction

For most patients with inflammatory bowel disease (IBD) including Crohn's disease and ulcerative colitis, the peak age at onset is between 20 and 40 years [1]. However, a minority of IBD patients have very early onset IBD (very early onset inflammatory bowel disease, VEOIBD) with onset at age 5 or younger, and disease in these children is unusually severe and may include extra-intestinal manifestations [2]. Whereas the heritability of adult IBD is assumed to be polygenic, VEOIDB is enriched for monogenic lesions with large effects on the encoded protein, often resulting in complete loss of protein function [2–4]. Mendelian forms of VEOIBD can be due to bi-allelic mutations in *IL10RA* or *IL10RB*, genes encoding the two chains of IL-10 receptor [5]. Along with mutations affecting the IL-10 cytokine itself [6], these mutations abrogate IL-10-dependent signaling and result in severe immune dysregulation [5, 6]. Affected children typically develop severe colitis and perianal lesions within the first weeks or months of life [6]. Early genetic diagnosis is necessary to perform hematopoietic stem cell transplantation (HSCT) [5, 6], and in parts of the world where genetic testing is unavailable to most patients, this disease may be under-diagnosed. Many of the reported patients with disease-causing mutations in *IL10RA* or *IL10RB* have been from consanguineous families [5, 6]. Here, we report a case of complete autosomal recessive IL-10Rβ deficiency caused by a novel mutation in *IL10RB* in a non-consanguineous family. We used low-pass whole genome sequencing data to assess haplotypes surrounding *IL10RB* in several members of the pedigree and estimated the most recent common ancestor, establishing the IL-10Rβ W40X allele as a founder mutation in the isolated population to which this patient belongs.

Methods

Preparation of peripheral blood mononuclear cell (PBMC) and B lymphocytic cell lines (B-LCL)

Following informed consent of all study participants, whole blood samples from healthy controls and patients were collected by venipuncture and then diluted 1:1 in

Received 24 May 2023; Revised 27 June 2023; Accepted for publication 27 July 2023

sterile Dulbecco's Phosphate Buffered Saline (PBS; Sigma #RNBH2262) and 2% fetal bovine serum (FBS). Separation of PBMC was done using Ficoll-Paque (GE #14004038) and SepMate tubes (Stemcell Technologies #85450). One million PBMC were resuspended in 1 ml RPMI 1640 medium (Gibco #11875-093) with 10% FBS and 1% antibiotic mix (Fisher #501015476) and mixed with 1 mL Epstein–Barr virus supernatant produced from B95-8 cells and 1 μg/ml of cyclosporine A (Sigma #C1832). Cells were cultured at 37°C, 5% CO_2 for 24 h, then half the media was removed and replaced with fresh EBV supernatant and cyclosporine A. Culture volume was increased as needed with RPMI 1640 with 10% FBS and 1% antibiotic mix.

Flow cytometry

B-LCL were stained with PE isotype control antibody (Biolegend, #400213) or PE anti-human CD210b (IL-10Rβ) antibody (Biolegend, #S17009F) diluted 1:50 in PBS with 2% heat-inactivated flow cytometry standard file (FCS) for 30 min at room temperature. Cells were washed twice by centrifugation at 300g for 5 min and the supernatant was removed. Cell pellets were resuspended in PBS with 2% heat-inactivated FCS and data was acquired on the Becton, Dickinson and Company (BD) Biosciences LSR-II flow cytometer (Becton, Dickinson and Company). Analysis was done in FlowJo v10 and GraphPad Prism software.

Cytokine stimulation and western blotting

B-LCL cells were either left untreated or were stimulated for 30 min with either IL-10 (200 ng/ml, R&D Systems #1064-IL-010) or IFN-α2a (10^5 units/ml, R&D Systems #111001). Cells were then pelleted and lysed in cold RIPA lysis buffer with protease and phosphatase inhibitors (VWR #PI88667) for 30 min on ice, then centrifuged at 12 000g for 15 min. Supernatant, containing protein, was collected and quantified using DC Protein Assay Kit II (Biorad, Catalog #5000112) based on manufacturer's instructions, equal amounts of protein were loaded on 12% gels for SDS–PAGE and then transferred to PVDF membranes. Membranes were blocked with TBS-T containing 0.1% tween and 5% non-fat dry milk, then probed with the following antibodies in blocking buffer: rabbit phospho-STAT3 (Y705; Cell signaling #9145S), mouse total STAT3 antibody (Cell signaling #9139S), or mouse GAPDH antibody (Thermo #AM4300), followed by HRP-conjugated secondary antibodies anti-rabbit IgG (Invitrogen #31460) or anti-mouse IgG (Invitrogen, 31430) as appropriate. Blots were developed using an enhanced chemiluminescence (ECL) substrate (Thermo #32209) and imaged using an Amersham Imager 680.

Cytometry by time-of-flight (CyTOF)

Approximately 5×10^6 PBMCs were stained with Cell-ID Cisplatin-195Pt to discriminate dead cells. PBMCs were then FcR blocked with Human TruStain FcX (Biolegend #422302), stained with the antibody mix as shown in Supplementary Table S1, fixed with 1.6% paraformaldehyde, and stained with Cell-ID intercalator-Ir. Stained PBMCs were analyzed in a Helios CyTOF 3.0 (Fluidigm) following the manufacturer's instructions at the Cancer and Immunology Core at Vanderbilt University. The data were exported as an FCS and normalized using EQ-Four calibration beads standards (Fluidigm # 201078) following the manufacturer's protocol. For multidimensional analysis, the data were pre-gated to remove dead cells and debris, then gated for CD45 + cells using FlowJo 10.7.2 (Becton, Dickinson & Company). The pre-gated data were exported as FCS files and then imported into RStudio. We used the package CATALYST [7] to arcsine transform marker intensities with a cofactor of five and performed subsequent analysis. Unsupervised clustering was performed using FlowSOM [8], and data representation was performed using the R package ggplot2. Manual gating was performed in FlowJo. Frequencies of various populations were exported from FlowJo and analyzed using Prism 9 (GraphPad Software).

DNA extraction and Sanger sequencing

Genomic DNA was isolated from whole blood or saliva. Polymerase chain reaction (PCR) was performed using primers F1 5′-CTGGGCTCATTCATCTGGCT-3′ and 5′-GGCACAGCATGAGGTTACCA-3′ according to Taq PCR kit manufacturer protocol (New England Biolabs # E5000S) and confirmed by gel electrophoresis. Nested PCR was performed using primers F2 5′- GCAGCTCAAATGGGACTCGT-3′ and R2 5′-GCCAATAGTGAGGCCAGACC-3′ and confirmed by gel electrophoresis. Sanger sequencing was performed using primers F3 5′-TCTAGACTCCTCAGCACAGC-3′ and R3 5′-GAGCTGTGAAAGTCAGGTTC-3′ and BigDye Terminator v3.1 (Thermo #4337458) then analyzed using an ABI3130xL capillary DNA analyzer and SnapGene software.

Estimation of allele age

Illumina low-pass whole genome sequencing was performed on genomic DNA samples obtained from six individuals in the family pedigree, including the proband, who were Sanger-confirmed to harbor the *IL10RB* W40X mutation. Raw reads were aligned to the human reference genome build GRCh38/hg38 using Burrows-Wheeler Aligner (0.7.17) [9]. PCR duplicates were subsequently identified in the aligned reads, and base quality scores were recalibrated, in accordance with the GATK Best Practices Workflow. Genomic variant call format files from all six individuals underwent joint variant calling using GATK's HaplotypeCaller (4.2.2.0). Finally, variant quality scores were recalibrated for both single nucleotide polymorphisms and indels. After variant calling was completed, the resulting VCF was pruned using VCFtools (0.1.15) for genotypes with any level of missingness across the six individuals, a minor allele count of at least 3, the minimum quality score of 30, and a minimum read depth of 5. From this pruned VCF, chromosomal haplotypes for chr21 were phased with SHAPEIT4 (4.2.2) [10], using 1000 Genomes 30× on GRCh38 phased calls for 3202 samples as a reference panel. Then, from the resulting phased VCF, hap/sample files were generated with bcftools (1.8). Using R (4.1.0), the hap file was reformatted as a 13-column text file, containing the chr21 coordinate and phased variant calls for each of the 12 phased chromosomes (two per individual) at that site. Phased variant calls were manually spot-checked for concordance with the aligned reads using IGV (2.9.4). The length of the left and right shared haplotype arms were calculated for each individual by finding the difference in genetic position (in cM) between the farthest shared variant and the genetic position of the W40X stop-gain mutation. The respective lengths of the left (upstream

of the mutation) and right (downstream of the mutation) arms served as inputs for the Mutation_age_estimation.R script [11]. We selected a confidence coefficient of 0.95 and excluded the chance sharing correction.

Results

Clinical case and identification of *IL10RB* mutation

A male patient presented with a history of recurrent diarrhea and eczema since the first month of life. Before age 2 years, the patient had one severe respiratory tract infection, one episode of sinusitis, two episodes of oral candidiasis, chronic diarrhea, and showed developmental delay. At age 2 years, an endoscopy revealed the presence of cryptitis and microabscesses in the cecum and transverse colon, and cryptitis, abscesses, and granuloma in the descending colon and rectum. The patient also had peri-anal fistula and unusual pigmentation of hair, skin, and teeth (Fig. 1A). DNA from this patient was sent for analysis using a gene panel (Invitae primary immunodeficiency panel), which revealed a novel homozygous c.120G > A variant in *IL10RB*, resulting in the creation of the premature stop codon W40X with CADD score 41 [12] and predicted to truncate the IL-10Rβ protein prior to its transmembrane domain. Sanger sequencing of DNA from each parent confirmed autosomal recessive inheritance of this variant (Fig. 1B). Since IL-10Rβ-deficient patients require allogeneic (HSCT) [5], this procedure was recommended, but unfortunately the patient's status deteriorated and he died before transplantation could be done.

Functional tests confirm complete IL-10Rβ deficiency

IL-10 is an anti-inflammatory cytokine secreted by a variety of cells, including regulatory T cells [13]. IL-10 limits excessive immune responses by inhibiting the secretion of pro-inflammatory cytokines such as IL-12 and TNF-α [14]. The IL-10 receptor is composed of two molecules of IL-10Rα and two molecules of IL-10Rβ. IL-10Rβ is a subunit for several other cytokines also, such as IL-22 and IL-26 [13]. The W40X mutation was in the extracellular domain of the protein and was predicted to severely impair or abolish protein expression. B-LCL were generated for the patient, his mother, and healthy controls. As expected, flow cytometry results indicated that cells of the W40X homozygous patient had no IL-10Rβ protein expression, whereas the patient's heterozygous mother had reduced IL-10Rβ protein expression relative to healthy controls (Fig. 1C and D). While healthy control and W40X heterozygous B-LCL responded to IL-10 stimulation by phosphorylating STAT3, cells from the patient showed no response to IL-10 (Fig. 1E). Interferon-α2a was used as a positive control for pSTAT3 induction (Fig. 1E). These results confirm that this patient had complete autosomal recessive IL-10Rβ deficiency.

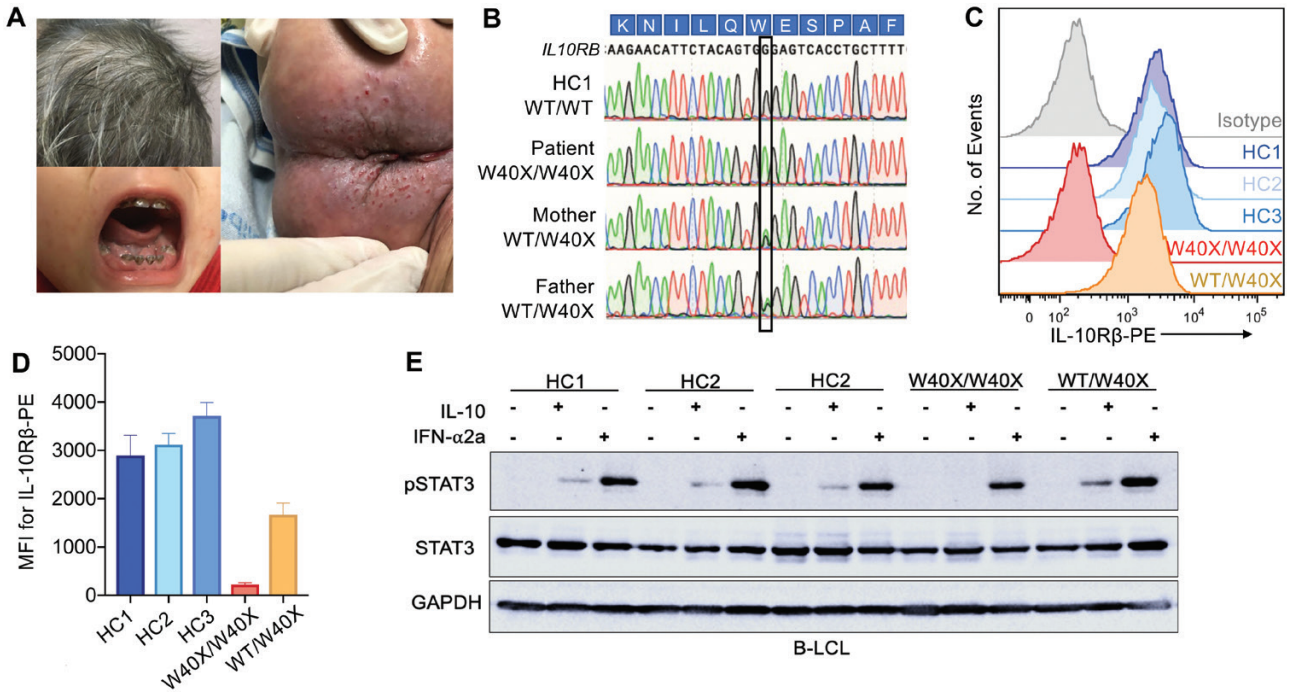

Figure 1. Novel mutation W40X causes complete autosomal recessive IL-10Rβ deficiency. (A) The patient presented with several symptoms of immune dysregulation, including chronic diarrhea with perianal fistula, and chronic eczema. The patient also displayed unusual pigmentation in his hair and teeth. (B) Sanger sequencing of genomic DNA from the patient and each of his parents showed a novel G > A mutation in *IL10RB* resulting in the coding change W40X. This mutation was homozygous in the patient, and heterozygous in each parent. A healthy donor sample (HC1) was used as a control. (C) Flow cytometry was used to assess the cell surface expression of IL-10Rβ in B lymphoblastoid cells lines generated from three different healthy controls (HC1-3), the patient (W40X/W40X) and the patient's mother (WT/W40X). A PE-conjugated isotype control antibody was used to indicate background or non-specific signals. (D) Mean fluorescence intensity (MFI) for IL-10Rβ-PE was calculated for data shown in C, and $n = 4$ other replicate experiments. (E) Cells from three different healthy controls (HC1-3), the patient (W40X/W40X), and the patient's mother (WT/W40X) were either left unstimulated or were stimulated for 30 min with IL-10 (200 ng/ml) or IFN-α2a (10^5 units/ml). Western blots show phosphorylated STAT3 (pSTAT3), total STAT3, and GAPDH as a protein loading control

Cellular phenotypes in IL-10Rβ deficiency

Routine immunological workups typically done in hospital settings have not revealed marked differences when comparing patients with IL-10R defects to healthy age-matched controls [15]. The reported frequency of CD4 + regulatory T cells (Tregs) in the blood of IL10R-deficient patients was comparable to healthy subjects [16]. However, there is some evidence of exaggerated Th17 responses in the setting of IL-10R deficiencies. Naïve CD4 T cells from IL10R-deficient patients proliferated more and produced higher levels of IL-17 relative to naïve CD4 T cells from healthy controls [16]. In addition, these patients had elevated levels of colonic *RORC* RNA expression (upregulated in IL17A-producing T cells) compared to healthy controls, and this same phenotype was observed in a larger cohort of patients with active Crohn's disease [16]. These data suggest that in humans, IL10R-dependent signals regulate Th17 differentiation in both peripheral and mucosal compartments [16]. Using CyTOF, we broadly profiled the immune landscape of our IL-10Rβ-deficient patient and compared his data to those of healthy adult controls ($n = 13$) and healthy pediatric controls ($n = 2$). In agreement with previous data [15], we did not identify a broadly disrupted immune cell profile in this IL-10Rβ-deficient patient (Fig. 2A and B). However, we did identify reduced frequencies of total CD4 + and CD8 + T cells, CD4 + CD8 + double-positive T cells, and low mucosal-associated invariant T cells and natural killer cells in this patient (Fig. 2C). Although total B cells were not reduced in frequency (Fig. 2C), the relative frequencies of both switched and non-switched memory B cells were reduced, and the frequency of naïve B cells was elevated, in this patient (Fig. 2D). Also in agreement with previous publications [16], we observed a normal frequency of Treg but an elevated frequency of Th17 cells in this patient (Fig. 2E).

Estimating mutation age

The presence of the same private IL-10Rβ W40X mutation in the heterozygous state in each of our patient's unrelated parents led us to investigate a possible founder effect. The patient's family is part of an indigenous group living in a remote region of Ecuador with a current population of <15 000. We performed Sanger sequencing of this variant in 14 members of the patient's extended family and found five heterozygous individuals (Fig. 3A). Next, we estimated the age of the IL-10Rβ W40X mutation based on the genetic length of ancestral haplotypes shared between the 5 WT/W40X individuals and the proband using low-pass whole genome sequencing data. We used the Gamma method for estimating mutation age, which infers ancestral haplotype segment lengths from high-density single nucleotide polymorphisms data (Fig. 3B) and has shown reliability for small sample sizes, typical of rare mutation studies [11]. This analysis showed the predicted age of the W40X mutation is 73 generations (95% confidence interval (CI), 27–148). Assuming an average generation length of 20–25 years, this indicates the W40X mutation is approximately 1460–1825 years old. These data suggest that IL-10Rβ W40X is a founder mutation within the indigenous Ecuadorian population in this region.

Discussion

This study has identified a novel W40X mutation resulting in complete autosomal recessive IL-10Rβ deficiency in a child of non-consanguineous parentage. The W40X mutation results in loss of IL-10Rβ surface expression and loss of IL-10-dependent signaling in patient cells. In terms of immunophenotype, this patient showed reduced overall frequencies of CD4 + and CD8 + T cells, and within the CD4 + compartment had an elevated frequency of Th17. We also report reduced generation of memory B-cell populations and some innate-like T cells in this patient. To date, there are relatively few publications reporting comprehensive immunophenotyping in patients with IL-10R deficiencies, partially owing to the exigency of HSCT to save these patients' lives. Out data reinforce previous reports of normal Treg but dysregulated Th17 differentiation in the setting of IL-10R deficiency [15, 16] and further suggest additional, subtle defects in the generation of B-cell memory and development or survival of some innate-like T-cell populations. Additional work with more IL-10R patients' samples is needed to assess the generalizability of these findings.

This patient's family belongs to an indigenous group living in a sparsely populated area of Ecuador. Using genome-wide sequencing data, we determined that this allele is part of a haplotype that originated approximately 1460–1825 years ago in this population. Consanguinity and endogamy increase the risk for autosomal recessive inborn errors of immunity (IEI), and many novel IEI-causing genetic variants have been discovered via the study of consanguineous kindreds [17, 18]. Globally, couples related as second cousins or closer and their progeny are thought to account for approximately 10% of the population [19]. In some populations, up to 50% of marriages may be consanguineous [19]. In other populations, more distant parental relatedness may arise from small and relatively isolated populations, or as a consequence of founder effects in tight-knit groups [20, 21]. Genetic variants causing autosomal recessive IEI may result from distant, and previously unrecognized, forms of parental relatedness. For example, a splicing mutation in *CTPS1* leading to autosomal recessive immunodeficiency was identified in five kindreds from the northwest region of England [22]. This allele arose from a founder effect, though the age of the allele was not determined [22]. The *IFNGR2* G141R mutation causing mycobacterial susceptibility was found in two unrelated Turkish patients, who were later found to have a common haplotype with the most recent common ancestor estimated at 103 generations ago (95% CI, 33–491) [23]. Autosomal recessive *DIAPH1* deficiency in four unrelated and non-consanguineous Finnish families was shown to be due to homozygosity for a splicing variant estimated to have arisen from a shared ancestral haplotype 17.9 generations ago (95% CI, 4.3–32.5) [24]. Finally, there is another known example of IL-10Rβ deficiency due to a founder effect. A previous study reported three unrelated Portuguese children with VEOIBD, all sharing an exon 3 deletion in *IL10RB* [25]. Genotyping of microsatellites surrounding this mutation revealed that all three patients shared a common haplotype, pointing to a founder deletion inherited from a common ancestor 400 years ago [25]. These findings suggest that, alongside consanguinity and endogamy, the existence of a more distant common ancestor or founder effect may underlie many cases of autosomal recessive inborn errors of immunity. Expanded population-level genetic testing may help to shed light on this possibility and may identify additional cases of IL-10Rβ deficiency, enabling the timely provision of life-saving HSCT treatment.

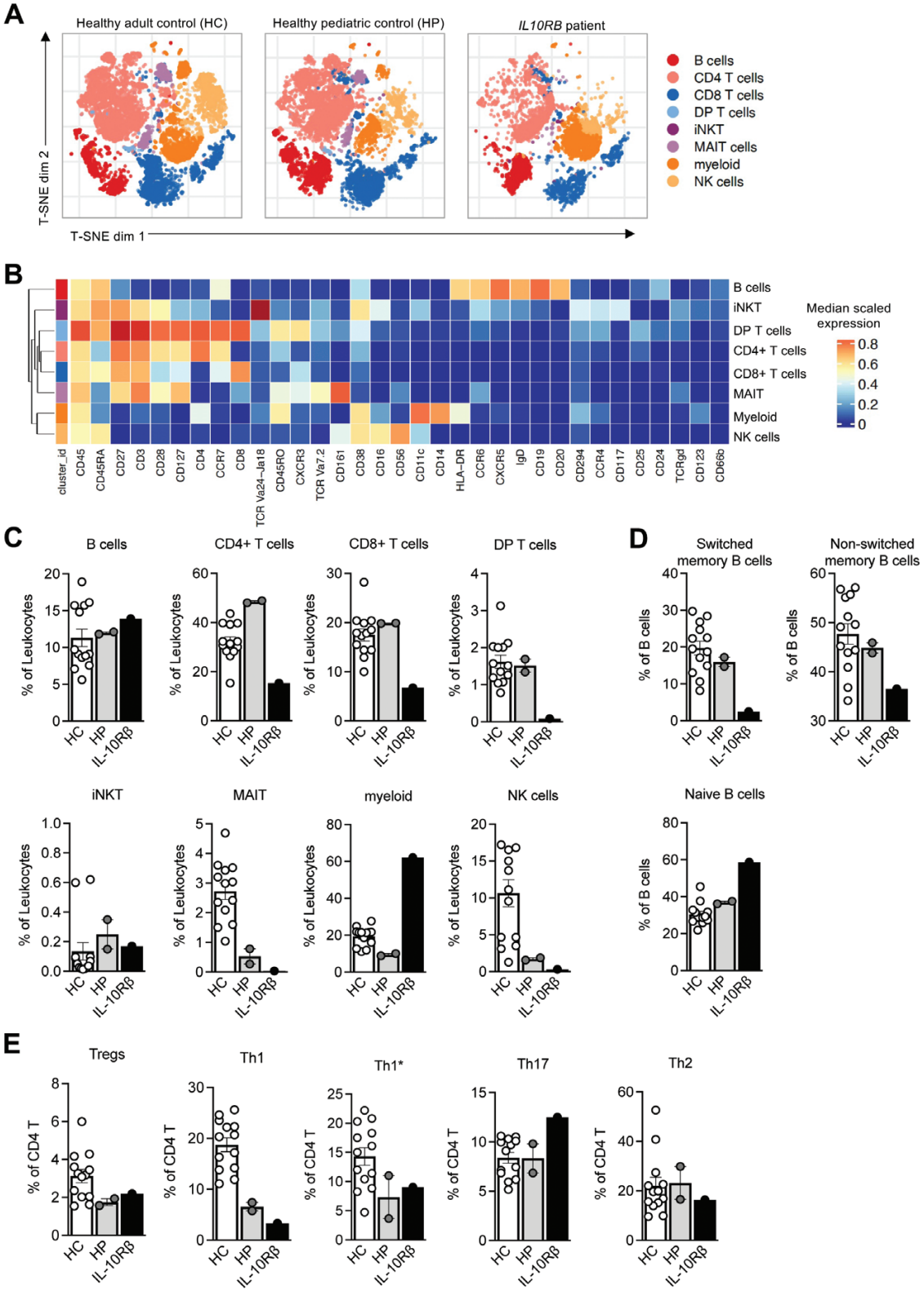

Figure 2. IL-10Rβ deficient patient shows reduced overall CD4 and CD8 T-cell frequencies, as well as more subtle defects in T helper, innate-like T, and memory B-cell populations. The immune landscape of IL-10Rβ deficiency was broadly assessed using a 33-antibody panel by CyTOF. The patient's sample was compared against samples from healthy adult control (HC, $n = 13$) and healthy pediatric donors (HP, $n = 2$). (A) T-distributed stochastic neighbor embedding plots depict the results of unbiased clustering of total live CD45 + leukocytes from one HC, one HP), and our *IL10RB* patient. Data were downsampled to illustrate results from 10^4 cells per person. (B) Median expression heatmap of the markers shown under the graph, for the cell populations shown in A. (C) The same raw data used in parts A–B were manually gated to identify eight cell populations of interest, corresponding to the eight broad clusters of cells identified in part A, to validate the results of unbiased clustering. The relative frequency of each cell type, as a percentage of CD45 + leukocytes, is shown for each individual. HC, $n = 13$, HP, $n = 2$), and our IL-10Rβ deficient patient (IL-10Rβ). (D) Sub-gating of B cells based on expression of CD27 and IgD was used to define switched memory (IgD−CD27+), non-switched memory (IgD + CD27+), and naïve (IgD + CD27−) B cells. (E) CD4 helper T-cell subset frequencies were assessed. Tregs (CD25 + CD127−), Th1 (CCR6−CXCR3+), Th1* (CCR6 + CXCR3+), Th17 (CCR6 + CXCR3−), and Th2 (CCR6−CXCR3−) subsets are shown

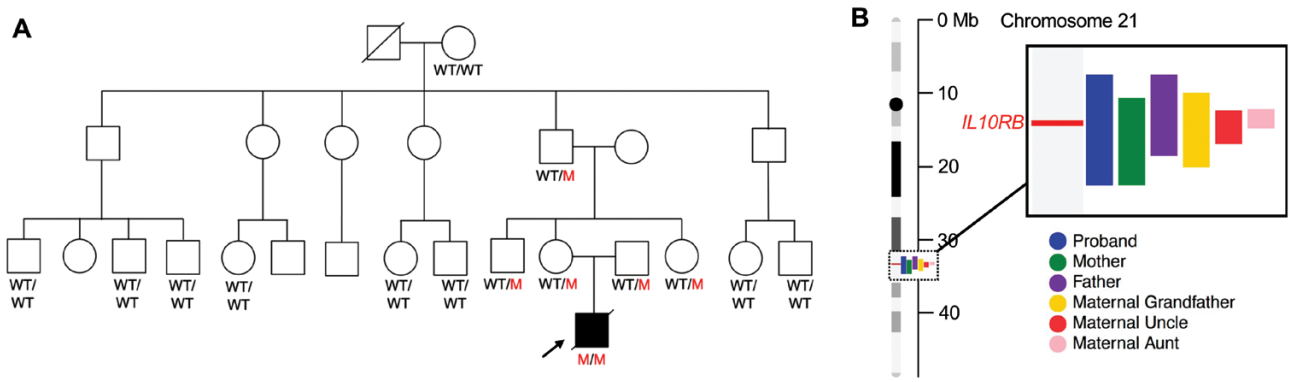

Figure 3. Familial segregation of the IL-10Rβ W40X mutation, and length of shared haplotypes. (A) Genomic DNA samples were collected from members of the patient's extended family and Sanger sequencing was used to determine that five individuals were heterozygous for the IL-10Rβ W40X mutation. Low-pass whole genome sequencing was performed on these five individuals, plus the proband (indicated by an arrow). (B) Phased haplotype lengths on chromosome 21 were compared for all W40X mutation carriers, and these data were used to estimate the age of the ancestral haplotype

Supplementary Data

Supplementary data is available at *Clinical and Experimental Immunology* online.

Ethics Approval

This work was conducted under approved IRB protocols at The Johns Hopkins Bloomberg School of Public Health and Vanderbilt University Medical Center.

Conflict of Interests

The authors declare no competing financial interests.

Funding

The authors acknowledge funding from the Johns Hopkins Digestive Diseases Basic and Translational Research Core Center (P30DK089502) and Vanderbilt University Medical Center's Digestive Disease Research Center (P30DK058404).

Data Availability

All data will be made available as institutional guidelines allow, by request, by contacting the corresponding author at janet.markle@vumc.org.

Author Contributions

Z.M., Q.L., and J.M.C. performed DNA extractions, sequencing, and functional experiments. M.J.B. analyzed WGS data and performed allele age calculations. S.B. performed CyTOF data analysis in RStudio. M.A.C. and L.A.P. compiled clinical data, arranged sample collections, and contributed to study design. J.G.M. contributed to study design, data acquisition, data interpretation, drafting figures and writing the manuscript. All authors have reviewed and approved the manuscript.

Patient Consent

Parental informed consent for this research and its publication was obtained.

Permission to Reproduce

Not applicable.

Clinical Trial Registration

Not applicable.

References

1. Uhlig HH. Monogenic diseases associated with intestinal inflammation: implications for the understanding of inflammatory bowel disease. Gut 2013, **62**, 1795–805. doi:10.1136/gutjnl-2012-303956.
2. Uhlig HH, Schwerd T, Koletzko S, Shah N, Kammermeier J, Elkadri A, et al. The diagnostic approach to monogenic very early onset inflammatory bowel disease. Gastroenterology 2014, **147**, 990–1007.e3. doi:10.1053/j.gastro.2014.07.023.
3. Schwerd T, Bryant RV, Pandey S, Capitani M, Meran L, Cazier J-B, et al. NOX1 loss-of-function genetic variants in patients with inflammatory bowel disease. Mucosal Immunol 2018, **11**, 562–74. doi:10.1038/mi.2017.74.
4. Uhlig HH, Muise AM. Clinical genomics in inflammatory bowel disease. Trends Genet 2017, **33**, 629–41. doi:10.1016/j.tig.2017.06.008.
5. Glocker EO, Kotlarz D, Boztug K, Gertz EM, Schäffer AA, Noyan F, et al. Inflammatory bowel disease and mutations affecting the interleukin-10 receptor. N Engl J Med 2009, **361**, 2033–45. doi:10.1056/NEJMoa0907206.
6. Kotlarz D, Beier R, Murugan D, Diestelhorst J, Jensen O, Boztug K, et al. Loss of interleukin-10 signaling and infantile inflammatory bowel disease: implications for diagnosis and therapy. Gastroenterology 2012, **143**, 347–55. doi:10.1053/j.gastro.2012.04.045.
7. Nowicka M, Krieg C, Weber LM, Hartmann FJ, Guglietta S, Becher B, et al. CyTOF workflow: differential discovery in high-throughput high-dimensional cytometry datasets. F1000Research 2019, **6**, 748. doi:10.12688/f1000research.11622.1.
8. Van Gassen S, Callebaut B, Van Helden MJ, Lambrecht BN, Demeester P, Dhaene T, et al. FlowSOM: using self-organizing maps for visualization and interpretation of cytometry data. Cytom. Part A 2015, **87**, 636–45. doi:10.1002/cyto.a.22625.
9. Li H, Durbin R. Fast and accurate short read alignment with Burrows-Wheeler transform. Bioinformatics 2009, **25**, 1754–60. doi:10.1093/bioinformatics/btp324.
10. Delaneau O, Zagury JF, Robinson MR, Marchini JL, Dermitzakis ET. Accurate, scalable and integrative haplotype estimation. Nat Commun 2019, **10**, 5436. doi:10.1038/s41467-019-13225-y.

11. Gandolfo LC, Bahlo M, Speed TP. Dating rare mutations from small samples with dense marker data. Genetics 2014, **197**, 1315–27. doi:10.1534/genetics.114.164616.
12. Rentzsch P, Witten D, Cooper GM, Shendure J, Kircher M. CADD: Predicting the deleteriousness of variants throughout the human genome. Nucleic Acids Res 2019, **47**, D886–94. doi:10.1093/nar/gky1016.
13. Moore KW, Malefyt RDW, Robert L, Garra AO. Interleukin-10 and the interleukin-10 receptor. Mol Cell Biol 2001. doi:10.1146/annurev.immunol.19.1.683.
14. Couper KN, Blount DG, Riley EM. IL-10: the master regulator of immunity to infection. J Immunol 2008, **180**, 5771–7. doi:10.4049/jimmunol.180.9.5771.
15. Glocker EO, Kotlarz D, Klein C, Shah N, Grimbacher B. IL-10 and IL-10 receptor defects in humans. Ann N Y Acad Sci 2011, **1246**, 102–7. doi:10.1111/j.1749-6632.2011.06339.x.
16. Shouval DS, Konnikova L, Griffith AE, Wall SM, Biswas A, Werner L, et al. Enhanced TH 17 responses in patients with IL10 receptor deficiency and infantile-onset IBD. Inflamm Bowel Dis 2017, **23**, 1950–61. doi:10.1097/MIB.0000000000001270.
17. Al-Mousa H, Al-Saud B. Primary immunodeficiency diseases in highly consanguineous populations from Middle East and North Africa: epidemiology, diagnosis, and care. Front Immunol 2017, **8**, 1–7. doi:10.3389/fimmu.2017.00678.
18. Al-Herz W, Aldhekri H, Barbouche MR, Rezaei N. Consanguinity and primary immunodeficiencies. Hum Hered 2014, **77**, 138–43. doi:10.1159/000357710.
19. Bittles AH, Black ML. Evolution in health and medicine Sackler colloquium: consanguinity, human evolution, and complex diseases. Proc Natl Acad Sci USA 2010, Suppl 1, 1779–86.
20. Ceballos FC, Joshi PK, Clark DW, Ramsay M, Wilson JF. Runs of homozygosity: windows into population history and trait architecture. Nat Rev Genet 2018, **19**, 220–34. doi:10.1038/nrg.2017.109.
21. Broman KW, Weber JL. Long homozygous chromosomal segments in reference families from the Centre d'Etude du Polymorphisme Humain. Am J Hum Genet 1999, **65**, 1493–500. doi:10.1086/302661.
22. Martin E, Palmic N, Sanquer S, Lenoir C, Hauck F, Mongellaz C, et al. CTP synthase 1 deficiency in humans reveals its central role in lymphocyte proliferation. Nature 2014, **511**, 370–70. doi:10.1038/nature13571.
23. Moncada-Vélez M, Martinez-Barricarte R, Bogunovic D, Kong X-F, Blancas-Galicia L, Tirpan C, et al. Partial IFN-γR2 deficiency is due to protein misfolding and can be rescued by inhibitors of glycosylation. Blood 2013, **122**, 2390–401. doi:10.1182/blood-2013-01-480814.
24. Kaustio M, Nayebzadeh N, Hinttala R, Tapiainen T, Åström P, Mamia K, et al. Loss of DIAPH1 causes SCBMS, combined immunodeficiency, and mitochondrial dysfunction. J Allergy Clin Immunol 2021, **148**, 599–611. doi:10.1016/j.jaci.2020.12.656.
25. Charbit-Henrion F, Bègue B, Sierra A, Hanein S, Stolzenberg M-C, Li Z, et al. Copy number variations and founder effect underlying complete IL-10Rβ deficiency in Portuguese kindreds. PLoS One 2018, **13**, e0205826. doi:10.1371/journal.pone.0205826.